HIGH SCHOOL EDITION
Journal of Student Research
Volume 13 Issue 1 (2024)

# Low-Cost, Manual Centrifuge for Separation of Particles from Water

Matthew Lavichant[1] and Rajeev Wahi[#]

[1]Flintridge Preparatory High School, USA
[#]Advisor

## ABSTRACT

Water separation is a critical process with far-reaching implications for the environment, public health, and various industries. Traditional water filtration methods are often limited to commercial use, posing challenges for individuals lacking access to clean water, or the equipment to separate particles suspended in water. In this study, we developed a spinning device for water separation through centrifugal and rotation force. Our goal was to create a device that could provide a low-cost alternative for removing contaminants from water. During the testing, we found that the device had a theoretical efficiency of 67% and longer separation times consistently produced significantly lower absorbance values in the visible range, indicating more effective particle removal. A computational model was also used to simulate the movement of particles under the influence of rotational forces, and showed that the smallest particle in this experiment (microplastics) can be theoretically moved by the rotational forces. This study underscores the promise of a manually powered spinning toy as an innovative and efficient tool for water separation and contaminant removal, holding the potential to address global water quality challenges.

## Introduction

Water separation plays a crucial role for the economy as it affects the environment, public health, and various industries. The process of water separation, which involves the removal of impurities and unwanted substances from water, yields clean and safe water for drinking and other uses. Water filtration is a common method used for water separation but is limited to commercial use. This is a challenge for individuals who don't have the necessary equipment to have access to clean water.

The water filtration technique is reverse osmosis which uses fine membranes in the micrometer ranges. The problem with reverse osmosis is that smaller microplastics are still difficult to remove and it's not cost efficient due to its high costs and ongoing maintenance requirement. Researchers have found that humans have consumed more than 70,000 particles of microplastic, with microplastic being detected in 80% of blood samples from human subjects [1]. The removal of microplastics is difficult and inefficient as it requires excess time and energy to mass purify water.

Recent studies have created a spinning toy to separate plasma by producing enough force to match electrically powered centrifuges [2]. With the same principle, the centrifugal force may be able to quickly separate a portion of clean water from contaminants such as dirt, sand, bacteria, and algae, leaving a smaller volume to filter manually. Moreover, this tool can be used to isolate desirable compounds in water and provide a low-cost method for water separation [3]. In this experiment, different variables were tested to find the optimal design for the spinning device. The final design uses a 14c m disk with a 100-130 cm string resulting in 67% efficiency.

[1] Archdall, R. (2022, January 23). *Do water filters remove microplastics?*. My Water Filter. https://mywaterfilter.com.au/blogs/learning/do-water-filters-remove-microplastics]

[2] Bhamla, M. S., Benson, B., Chai, C., Katsikis, G., Johri, A., & Prakash, M. (2017, January 10). *Hand-powered ultralow-cost paper centrifuge*. Nature News. https://www.nature.com/articles/s41551-016-0009

[3] Centrifugal Separation. (n.d.). Retrieved from https://www.sciencedirect.com/topics/engineering/centrifugal-separation

# Methodology

## Prototype Model

Initially, a prototype spinning toy was created using standard fishing line and corrugated cardboard. The prototype had a total string length of 41 cm, an 8 cm cardboard disk with holes 2 cm apart and no handles. However, it exhibited instability during spinning.

**Figure 1.** Example of top-down view of unstable disk due to a large distance between holes. The disk does not stay perpendicular to the line and does not spin effectively.

## Optimization of Spinning Toys

Subsequently, multiple spinning toy models were developed, varying in dimensions. Cardboard disks with diameters of 6cm, 10 cm, and 14 cm were tested. These sizes were chosen based on a 10 cm base size from M. Prakash's work, with the other two sizes 4 cm apart for direct comparison. The center holes were spaced 2.5 mm apart. Braided fishing line, known for “supercoiling” [1] was used, and sturdy cardboard tube handles were added for improved grip. Each disk size was tested with two string lengths: 40-60 cm and 100-130 cm, determined in ranges due to the difficulty of precisely measuring the string length after knotting. The longer strings were expected to achieve higher spinning speeds as they allowed for more coiling, thus accumulating more potential energy. All materials used, except the fishing line, were sourced from used products. The estimated cost of each model ranged from $1.5 to $3.5, calculated based on the cost per square inch and cost per inch of materials.

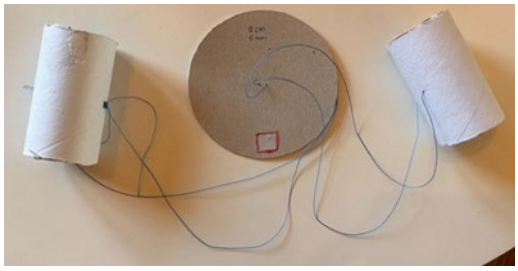

**Figure 2**. Example of cardboard model with 10 cm diameter and holes 5mm apart. 5mm proved to be too far apart, leading to the instability shown in Figure 1. Reflective tape and red outline was used to record the speed (rpm) with a laser tachometer.

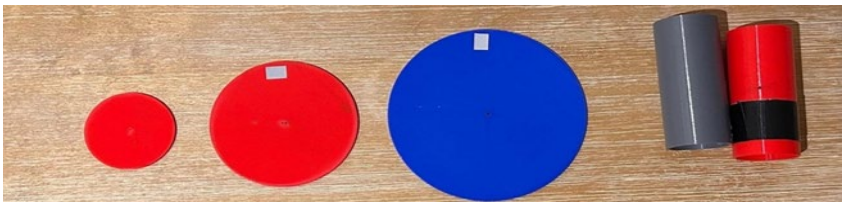

**Figure 3.** 3D printed PLA disks and handles. From left to right: 6 cm diameter disk, 10 cm diameter disk, 14 cm diameter disk, tubular handles.

Each model was suspended in the air and the disk was spun manually; then, the handles were pulled away from each other to achieve faster speeds. Once the string had been extended, tension was released from the handles and the string began to coil. The handles were pulled again once the disk stopped spinning. The top speeds (rpm) shown on a Soonkoda DT2234C$^{+}$ laser tachometer were recorded, and the number of pulls required to reach that top speed was also recorded. Each model was tested 3 times, and the average top speed from the 3 trials was calculated. It was observed that the string slowly cut through the cardboard between the two holes after testing, and once the holes had been connected, the spinning toy was defective. A 3D-printed model made of polylactic acid (PLA) was created to solve this issue. The 3D-printed models were limited to 3 designs (diameters 6 cm, 10 cm, and 14 cm; 2 holes of 1 mm diameter, 2.5 mm apart in the center; 2 mm thick). Using the 3D printing machine could cost around $1 per hour, and the entire process took around 5-6 hours, which gives an estimated cost of $5-6 for 3 disks and 2 handles.

These 3D printed models were tested in a similar manner to the cardboard disks. The top speeds of each disk were recorded after multiple pulls. The length of the fishing line was again hard to control, but all the tests had a length greater than 100cm.

## Particle Separation Experiments

To test the separation capabilities of the models, various solutions with different pollutants were used, including dirt, baby powder, algae from a local golf course, and polyethylene microplastics. Dirt contamination was assessed using a Total Dissolved Solids (TDS) water quality tool, while colorimetry was employed for the other three particle types. Before conducting experiments, control samples were collected for each pollutant. To contain dirt-contaminated water, clear plastic straws were sealed at one end, creating 3 cm long containers. These straws were attached to each side of a 10cm PLA disk using Gorilla Tape to maintain balance during spinning. Three time intervals (30 seconds, 1 minute, and 2 minutes) were chosen for spinning, following the range established by M. Prakash (0-2min). A total of 4 samples for each time interval were spun, resulting in 12 samples in the dirt category. Prior to spinning, the disk and fishing line were pre-coiled to ensure continuous rotation. After spinning, the straw containers were removed, and the end of each straw facing away from the disk's center displayed accumulated dirt. The opposite ends of the straws were removed, and 0.5ml of the contaminated water was extracted using a syringe.

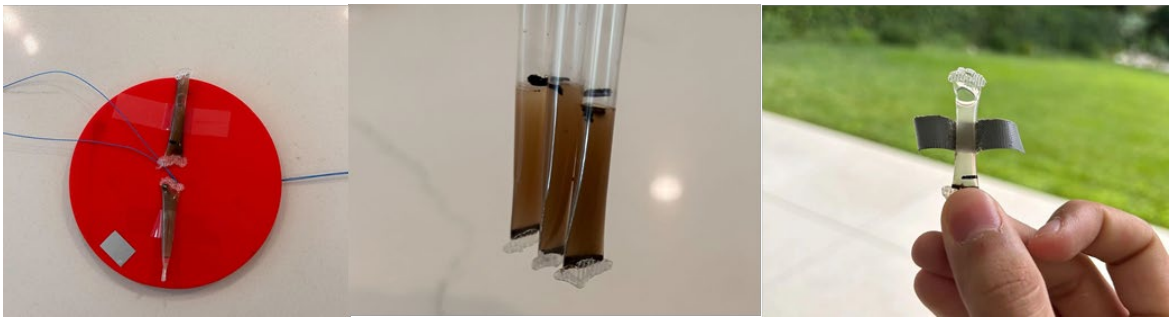

A B C

**Figure 4 (A).** Straw containers with dirt and water samples attached to the 10 cm diameter disk. Invisible tape was replaced with gorilla tape for experiments. 2 samples are on the visible side and 2 samples are on the back side.
**Figure 5 (B, C).** Before and after example of separated dirt and water sample in straw container after spinning. Dirt particles have accumulated near the thumb in the left picture.

Conductivity of water was measured using a YL-TDS2-A water quality tool. As the presence of dirt increased conductivity, samples were diluted with 10 ml of tap water to ensure compatibility with the tool's testing requirements. The TDS tool was calibrated against filtered tap water, which is approximately 35 ppm. It was calibrated to read 0 ppm for the dirt samples, and the ppm of each sample was recorded.

For microplastics, algae, and baby powder, a different approach was employed to improve efficiency. 1mL syringes were used to contain water samples, with control samples collected beforehand to establish a baseline. Four of these samples were attached to a 14cm PLA disk using gorilla tape, balanced on either side. The syringes were oriented with the tip facing away from the center and the flange toward the center, positioned around 0.7 cm from the center for fishing line clearance. Each group was spun for either 30 seconds or 1 minute. In total, there were 4 samples for each category for both time intervals. Following the spinning, 0.5 mL of each sample was extracted from the tip of the syringe, where particles theoretically accumulated due to centrifugal forces. Absorbance measurements were conducted with a Vernier COL-BTA Colorimeter interfaced with a LabQuest. The samples were transferred to cuvettes and diluted with 2mL of tap water to reach the necessary measurement height for the Colorimeter.

## Theoretical Efficiency Calculation

Experimental data and code was also used to simulate the movement of particles under the influence of forces produced by the spinning toy. The braided fishing line was run through the 14cm PLA disk and one side was looped around a stationary pole, while the other side was hooked to a digital luggage scale. The disk was coiled manually and then spun. Force was recorded in kilograms of force (kgf) using the digital luggage scale, and displacement was recorded by the difference between start and end position of the luggage scale. The Input work was calculated with these two values and the speed of the disk (rpm) was recorded to calculate theoretical efficiency using the equation: $\eta = \frac{K_{rot}}{Input\ work}$ . The disk weight (32.8g) was also used to calculate inertia. In short, the efficiency of the spinning toy was calculated by observing how much work was translated to the spinning force, and how fast the disk could spin.

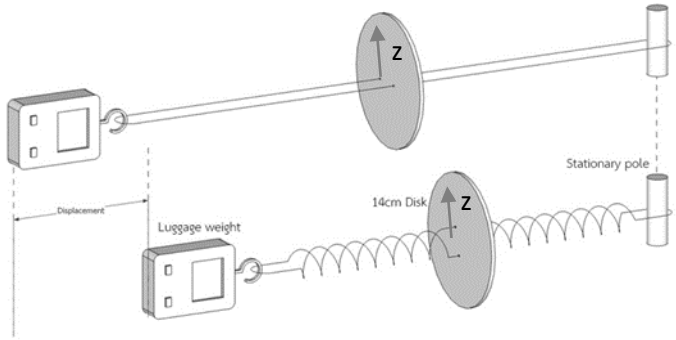


**Figure 6.** Diagram showing setup for theoretical efficiency calculation experiments. Spinning toy was pulled from the side of the luggage weight. Arrows on disk represent z axis for particle position.

To model the movement of the particles in a water medium, different forces were taken into account. Since the particles are very small, their motion in fluids is considered Brownian motion. To simulate the simplest form of Brownian motion, the particle trajectory undergoes a random walk with a Gaussian probability profile. The effect of thermal fluctuation was also taken into account by adjusting the variance of the distribution. To mimic the effect of a spinning disk, the centripetal force is introduced. Drag force is also included due to the water environment. Various parameters were set up such as step size, temperatures, viscosity, particle radius, etc. These parameters were adjusted depending on the particle type. Two functions were created: drag force and external centripetal force. The drag force function depends on the drag coefficient and the velocity. The external centripetal force depends on the velocity and the mass of the particle. The equation for the drag force is $F_{drag} = \gamma v$ where $\gamma = 6\pi\eta r$ where $\eta$ is the viscosity and r is the radius of the particle. The centrifugal force is $mz\omega^2$ where m is the mass of the particle, $\omega^2$ is angular velocity, and z is the position of the particle. The z position is indicated in Figure 6; z=0 is located at the center of the disk and increases as the particle moves away from the center while the disk is spinning. A for loop was created to extract the current position and velocity and update the velocity and position when taking account of drag and external centripetal force and storing the new position. It was assumed that gravity could be neglected since the particle weight was small compared to the centripetal force. Another assumption was that x and y are large enough that the particles will not hit the boundary.

## Results

The experimental investigation aimed to assess the effectiveness of a manually powered spinning toy for water separation and its potential application in removing various contaminants from water. This study explored the use of spinning disks made from both cardboard and 3D-printed PLA, with a focus on their spinning speeds and their capacity to separate different types of particles from water.

### Prototype Model

The initial prototype model constructed using standard fishing line and corrugated cardboard exhibited limitations in terms of its spinning performance. The prototype failed to remain perpendicular to the string during spinning. This resulted in an unsteady motion as the disk swung side to side, rendering it ineffective for our purposes. The absence of tubular handles on either side also contributed to the prototype's poor performance.

### Optimization of Spinning Toys

To improve the spinning toy's performance, various models with different dimensions and design modifications were tested. The modifications (non-corrugated cardboard, braided fishing line, and tubular handles) aimed to maximize the spinning speed (rpm) of the disks. 3D-Printed Models To address the issue of the string cutting through the cardboard, 3D-printed models made of polylactic acid (PLA) were introduced. These 3D-printed models were tested similarly to the cardboard disks but with 3D-printed handles instead of cardboard handles.

Two tables were created from the initial experiments of recording the top speed (rpm) reached by cardboard disks and PLA disks of different sizes:

**Table 1.** Cardboard disk models. Disk diameter and length of the fishing line used is listed in the first column. Speed was measured by laser tachometer.

| Disk Diameter, line length | Speed | Total number of pulls |
|---|---|---|
| 10cm, 60.6cm | 7400 rpm | 12 pulls |
| 10cm, 108.6cm | 14454 rpm | 23 pulls |
| 14cm, 41.4cm | 5035 rpm | 20 pulls |
| 14cm, 118.9cm | 5206 rpm | 31 pulls |
| 6cm, 55.2cm | 24563 rpm | 11 pulls |
| 6cm, 103.4cm | 32337 rpm | 19 pulls |

**Table 2.** Top speeds (rpm) achieved by PLA disk models. Disk diameter and length of the fishing line used is listed in the first column. Speed was measured by laser tachometer.

| Disk Diameter, Rope length | Speed | Total number of pulls |
|---|---|---|
| 10cm, 93.5cm | 58320 rpm | 14 pulls |
| 14cm, 99.9cm | 8349 rpm | 17 pulls |
| 6cm, 92.3cm | 71492 rpm | 15 pulls |

The number of pulls was included to show how much energy was required to get the spinning devices to achieve a constant high speed. It was observed that the PLA disks were able to reach a much higher top speed than with the cardboard disks, and that generally a longer rope length also factored into the top speed achieved. Effects of these variables (rope length and disk size) were used as guiding principles in improving design. For example, it was observed that larger disks with greater inertia achieve lower maximum speeds, so it was hypothesized that smaller and lighter disks would reach a higher speed.

## Particle Separation Experiments

To evaluate the water separation capabilities of the spinning toys, different water samples contaminated with various particles were used. The TDS water quality tool was used to measure the dissolved ion concentrations in the water, reflecting changes due to the introduction of ions from the dirt particles. The ppm (parts per million) of each sample was recorded.

The ion concentration of the control sample was 113 ppm.

**Table 3.** Showing 4 TDS readings (ppm) of separated dirt and water samples with different time intervals. The mean ppm was calculated for each time interval. Longer time intervals have a lower ppm, and all means have a lower ppm than the control sample.

| Trail number | 30 sec (ppm) | 1 min (ppm) | 2 min (ppm) |
|---|---|---|---|
| 1 | 94 | 98 | 62 |
| 2 | 100 | 75 | 46 |
| 3 | 100 | 91 | 56 |
| 4 | 98 | 95 | 57 |
| Mean | 98 | 89.75 | 55.25 |

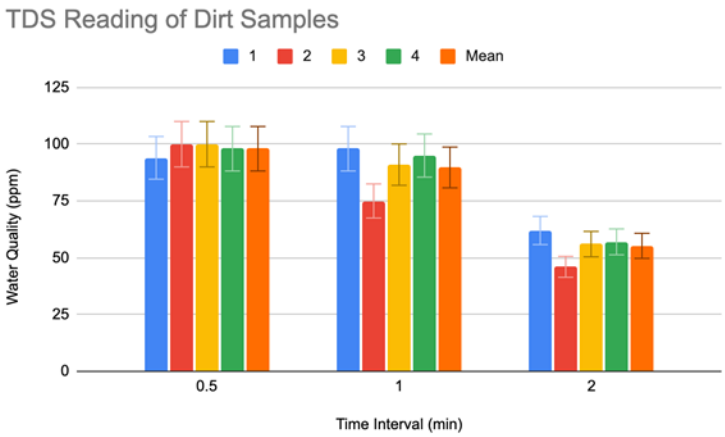


**Figure 7.** Bar graph showing results from Table 3. TDS readings for trails 1-4 are shown, as well as the mean. Mean of the 2 minute time interval is significantly different from means of 30 second and 1 minute time intervals. Error bars represent 10% of values.

The absorbance of the other samples was measured using a Vernier COL-BTA Colorimeter, with specific wavelengths chosen for each particle type to provide optimal readings. These measurements allowed for a quantitative assessment of particle removal efficiency. The absorbance of the microplastic samples was measured with a 470 nm wavelength of light, the algae samples were measured with a 430 nm wavelength of light, and the baby powder samples were measured with a 565 nm wavelength of light. These wavelengths were determined for each particle type because they provided the highest absorbance reading, allowing the different samples of each particle type to be compared easier.

From the separation experiments, a table of absorbance values was created:

**Table 4.** Showing absorbance of microplastic (MP), algae (A), and baby powder (BP) samples using Colorimeter. Readings for samples 1-4 are shown as well as mean. Microplastic samples were measured with 470 nm wavelength, algae samples were measured with 430 nm wavelength, baby powder samples were measured with 565 nm wavelength. 1 min time periods generally have lower absorbances.

| Sample Number | MP 30 sec | MP 1 min | A 30 sec | A 1 min | BP 30 sec | BP 1 min |
|---|---|---|---|---|---|---|
| 1 | 1.927 | 1.372 | 0.202 | 0.144 | 1.276 | 0.315 |
| 2 | 2.232 | 1.439 | 0.384 | 0.118 | 1.122 | 0.922 |
| 3 | 2.306 | 1.303 | 0.127 | 0.178 | 0.612 | 0.342 |
| 4 | 2.184 | 1.231 | 0.379 | 0.113 | 1.540 | 1.299 |
| Mean | 2.162 | 1.336 | 0.273 | 0.138 | 1.138 | 0.720 |

**Table 4. Showing absorbance of microplastic (MP), algae (A), and baby powder (BP) samples using Colorimeter. Readings for samples 1-4 are shown as well as mean. Microplastic samples were measured with 470 nm wavelength, algae samples were measured with 430 nm wavelength, baby powder samples were measured with 565 nm wavelength. 1 min time periods generally have lower absorbances.**

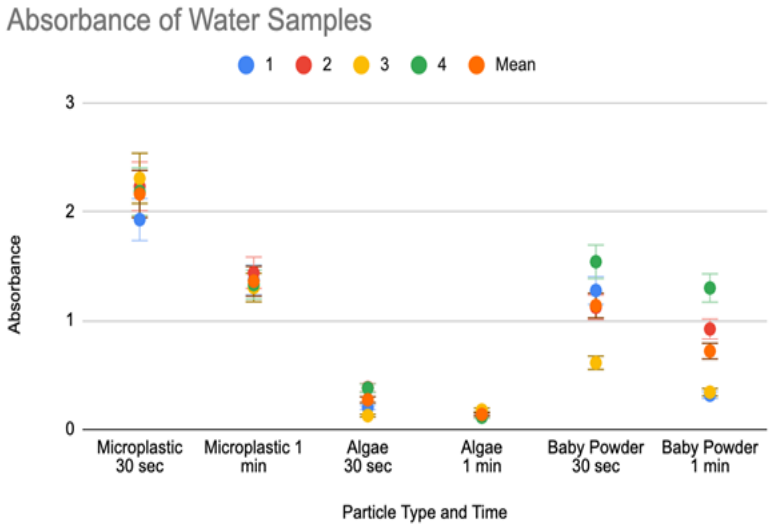


**Figure 8.** Scatterplot showing absorbance of water samples 1-4 in Table 4. Between each particle type, the mean 1 minute time interval had a significantly lower absorbance than the mean 30 second time interval.

The absorbances of the control samples, taken directly from the initial water samples were: 1.270 (microplastics), 0.470 (algae), and 0.939 (baby powder). It was observed that the absorbances of the controls were lower than those of the separated samples, but the 1 minute samples had a lower absorbance across all particle types.

## Theoretical Efficiency Calculation

In addition to experimental data, theoretical efficiency calculations were performed using the formula: $\eta = \frac{KE_{rot}}{Input\ work}$ where $KE_{rot}$ is the rotational kinetic energy and Input work is the work input from the spinning device. KE_rot = 1/2 * I * $\omega^2$, where KE_rot represents rotational kinetic energy, I is the inertia of the disk (1.13E-04), and ω is the angular velocity in radians per second (374.75). The angular velocity (ω) was calculated based on the recorded rpm. The results of these experiments and calculations will be presented and analyzed in the subsequent sections to assess the effectiveness of the spinning toy in water separation and its potential as a low-cost method for removing contaminants from water. The theoretical efficiency of the device was calculated as 67.1%.

**Table 5.** Showing data collected for theoretical efficiency calculations. Force was recorded by using luggage weight in kg and converted to Newtons. Start and end positions were determined by comparing the end of the string being pulled with a tape measure in the background. Displacement was converted to m for calculations.

| Trial number | Force (N) | Starting position (cm) | Ending position (cm) | Displacement (cm) |
|---|---|---|---|---|
| 1 | 21.48 | 93 | 34.5 | 58.5 |
| 2 | 19.02 | 99.5 | 37 | 62.5 |
| 3 | 23.05 | 100.5 | 35 | 65.5 |
| 4 | 20.2 | 107 | 42.5 | 64.5 |
| 5 | 19.71 | 98.5 | 43 | 55.5 |

| | | | | |
|---|---|---|---|---|
| 6 | 21.48 | 97 | 41 | 56 |
| 7 | 21.48 | 95.5 | 42.5 | 53 |
| 8 | 24.03 | 94 | 42 | 52 |
| 9 | 19.71 | 95 | 39.5 | 55.5 |
| 10 | 19.71 | 90 | 40.5 | 49.5 |
| Avg | 20.99 | | | 57.3 |

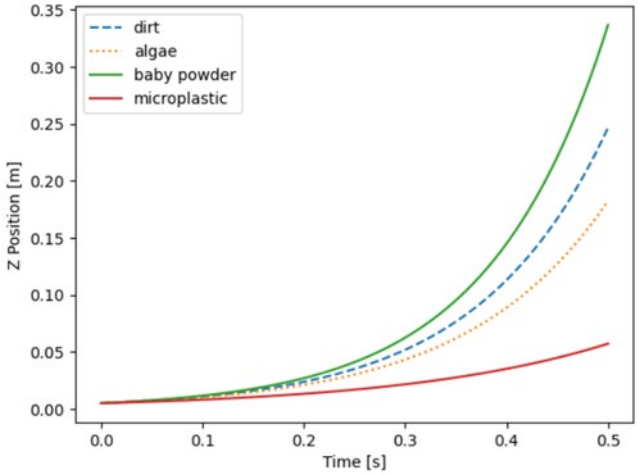


**Figure 9.** Z position (m) of the different particles over time as shown in Figure 6. Each line represents different particle types of movement over 0.5 second.

As seen in Figure 8, the simulation shows that baby powder will have the highest z-position movement while the microplastic will have the lowest movement. There is an exponential increase for the z position for all the particles. For dirt, algae, and baby powder, the growth rate is around 0.4 meters per second.

## Discussion

In the initial tests of the spinning toy, the prototype would be used to optimize and adjust subsequent models. Firstly, the regular fishing line was not as flexible, which greatly restricted the coiling ability of the prototype, and did not allow it to spin for long. Furthermore, the holes which allowed the fishing line to run through the disk were too far apart, and the disk did not remain stable during the spinning motion.

Various models with different dimensions were then tested. The incorporation of braided fishing line and sturdy cardboard tube handles significantly improved control and stability during spinning. The braided fishing line was especially effective in that it was able to coil to a great extent, with each pull and release cycle inputting more rotation energy, causing the fishing line to coil more. Additionally, the “supercoiling” phenomenon was much easier to achieve with the braided fishing line due to its flexibility. “Supercoiling” occurs “Since the strings are flexible (low bending stiffness), they wind beyond the geometric twist point, passing through a spectrum of helical twisting states” [2] as explained by M. Prakash et. al, and results in “a tightly packed ‘supercoiled’ state” [2]. While testing the cardboard models, it was observed that the fishing line cut through the cardboard between the holes where the fishing line was inserted. These holes were 2.5 mm apart, and once the line had cut completely through the cardboard, the model became dysfunctional. However, with the PLA models, this was not an issue as the PLA was strong enough to resist the abrasive forces of the coiling line in the center.

The results in Tables 1 and 2 indicate that a smaller disk is able to reach a higher speed, which makes sense as larger disks have more mass, leading to a larger inertia. The results also show that longer fishing lines allowed the model to reach a higher speed. Longer fishing line is able to coil to a greater extent, which builds up more potential energy to be released as the handles are pulled and the fishing line uncoils. The PLA disks were even more effective in reaching higher speeds (about 5.3 times faster for the 10 cm disk, 1.7 times faster for the 14 cm disk, and 2.5 times faster for the 6 cm disk). The 6cm disk even reached a speed greater than 70,000 rpm as shown in Table 2. With longer fishing lines, it is likely possible that the model can reach even higher speeds, perhaps greater than 100,000 rpm. It should be noted that a constant tension and release cycle needs to be maintained for the models to continue spinning. Also, the number of pulls required to reach the top speed may vary because of other factors such as increasing fatigue after multiple pulls.

Another important factor to consider is safety concerns with the spinning toy. The high rotational speed achieved by the PLA disks could potentially be a safety hazard. The braided fishing line has broken in previous tests, which led to the disks to fly in an unpredictable manner. The user must be extremely careful when spinning the models at high speeds, especially if the disk is in front of their face. However, this safety concern is addressed later when one end of the fishing line is tied to a stationary pole and the user is exerting force from one side, which moves them out of potential harm.

The results clearly indicate that the PLA disks, especially when equipped with longer strings, were capable of achieving much higher top speeds compared to cardboard disks, signifying an enhancement in performance due to the rigid structure that allowed the PLA disk to spin in a straighter plane.

Figure 7 and Table 3 show the TDS reading of the dirt samples and reveal there was no significant difference between the 30 second and 1 minute groups. There was a significant difference between the 1 minute group and the control, as well as between the 2 minute group and the rest of the groups, including the control. This affirms that the longer particles are under the influence of centrifugal and rotational forces created by the spinning disk, the more the particles tend to accumulate at the end of the container. The straw containers also proved to be very efficient as a low-cost alternative to more conventional containers such as test tubes.

Figure 8 and Table 4 reveal that there is a significant difference in the mean absorbance of the 30 second and 1 minute time intervals for each particle type. This shows that the amount of time particles are under the influence of centrifugal forces has an effect on the separation ability of the spinning toys. The difference between absorbance of these time periods is an indicator that the 30 second difference did affect the movement of particles, which implies that longer time intervals allow more particles to move with the forces produced by the rotational motion. Notably, the one-minute separation runs consistently produced lower absorbance values across all particle types, suggesting that longer separation times led to more efficient particle removal.

The theoretical efficiency of the spinning toy was calculated using rotational kinetic energy and input work calculations. The results yielded a theoretical efficiency of approximately 67.1%. While this theoretical efficiency is promising, it is essential to recognize that practical efficiency may vary due to factors such as fatigue or extraneous forces not considered during manual spinning. The data collected to calculate theoretical efficiency was limited in some ways. The target force was 2kgf, as higher target forces led to more instability in the force reading, but this is almost impossible to achieve every time with manual spinning.

As seen from figure 8, there is an exponential growth relationship between time and z position. This is due to the external centripetal force continuously being applied which causes an acceleration of particles in the outward direction. As the particles move further away from the center, they experience a greater force. It is also important to consider that an external centripetal force depends on the angular velocity and the particle mass; and depending on the range of particle size and density, certain types of particles could have a higher position.

The findings of this study have significant implications for water purification and environmental remediation. The spinning toy's ability to separate contaminants, particularly microplastics, suggests its potential

as a low-cost and eco-friendly method for water purification. Additionally, the use of 3D-printed PLA disks, coupled with longer ropes, demonstrates the feasibility of enhancing performance.

## Acknowledgments

I would like to thank my advisor for the valuable insight provided to me on this topic.

## References

[1] Archdall, R. (2022, January 23). *Do water filters remove microplastics?*. My Water Filter. https://mywaterfilter.com.au/blogs/learning/do-water-filters-remove-microplastics]
[2] Bhamla, M. S., Benson, B., Chai, C., Katsikis, G., Johri, A., & Prakash, M. (2017, January 10). *Hand-powered ultralow-cost paper centrifuge*. Nature News. https://www.nature.com/articles/s41551-016-0009
[3] Centrifugal Separation. (n.d.). Retrieved from https://www.sciencedirect.com/topics/engineering/centrifugal-separation
Rayleigh, Lord. (1917). On the Dynamics of Revolving Fluids. *Proceedings of the Royal Society of London. Series A, Containing Papers of a Mathematical and Physical Character*, *93*(648), 148–154. http://www.jstor.org/stable/93794
Pertiwi, A. P., & Saptarini, D. (2022). Microplastics characteristics of lorjuk solen sp. in east coastal waters of surabaya. IOP Conference Series.Earth and Environmental Science, 1095(1), 012034. doi:https://doi.org/10.1088/1755-1315/1095/1/012034
Arnold, J. M. (1869). Centrifugal Force. *Scientific American*, *20*(8), 118–118. http://www.jstor.org/stable/26031524
Bhamla, M. S., Benson, B., Chai, C., Katsikis, G., Johri, A., & Prakash, M. (2017, January 10). *Hand-powered ultralow-cost paper centrifuge*. Nature News. https://www.nature.com/articles/s41551-016-0009
Ece, E., Hacıosmanoğlu, N., & Inci, F. (2023). Microfluidics as a ray of hope for microplastic pollution. Biosensors, 13(3), 332. doi:https://doi.org/10.3390/bios13030332
Franco, J.J., Nagata, T., Okamoto, T. et al. An ultralow-cost portable centrifuge from discarded materials for medical applications. Sci Rep 13, 3081 (2023). https://doi.org/10.1038/s41598-023-30327-2